

Fast High-dimensional Approximate Nearest Neighbor Search with Efficient Index Time and Space

Mingyu Yang

The Hong Kong University of Science and Technology (Guangzhou)
myang250@connect.hkust-gz.edu.cn

Wentao Li

The Hong Kong University of Science and Technology (Guangzhou)
wentaoli@hkust-gz.edu.au

Wei Wang

The Hong Kong University of Science and Technology (Guangzhou)
weiwcs@ust.hk

ABSTRACT

Approximate K nearest neighbor (AKNN) search in high-dimensional Euclidean space is a fundamental problem with widespread applications. Vector quantization which maps vectors to discrete quantized code, can significantly reduce the space cost of AKNN search while also accelerating the AKNN search speed. The exclusive use of vector quantization without precise vectors leads to a substantial decline in search accuracy. Recent research RaBitQ addresses this issue by using geometry relation to enhance quantization accuracy and employing error bound for distance correction with precise vector. However, this method requires that the quantization bit must be equal to the vector dimension resulting in a fixed compression ratio which limits its efficiency and flexibility.

In this paper, we propose a new and efficient method MRQ to address this drawback. MRQ leverages data distribution to achieve better distance correction and a higher vector compression ratio. MRQ reduces the query latency based on a highly efficient distance computation and correction scheme. Our results demonstrate that MRQ significantly outperforms state-of-the-art AKNN search methods based on graph or vector quantization, achieving up to a 3x efficiency speed-up with only 1/3 length of quantized code while maintaining the same accuracy.

1 INTRODUCTION

K nearest neighbor search (KNN) in high-dimensional Euclidean spaces has recently received widespread research attention, due to its extensive applications in recommendation systems [48], data mining [10], information retrieval [40], and the Retrieval-Augmented Generation (RAG) of Large Language Models (LLMs) [38]. However, the curse of dimensionality [32] makes the exact K nearest neighbor search cost extremely high. Therefore, researchers have turned to studying approximate K nearest neighbor (AKNN) search [9, 13, 17–19, 21, 24, 29, 31, 49, 52, 58], sacrificing the accuracy for significantly improved search efficiency.

Vector quantization [27, 45] is a common technique for AKNN search, primarily aimed at reducing storage costs and enhancing retrieval efficiency. Among various quantization methods, Binary Quantization (BQ) [22, 26, 37, 39, 47] and Product Quantization [1–3, 5, 11, 23, 36, 53, 56] are widely applied in AKNN search. Binary Quantization (BQ) maps the original vectors into binary strings and calculates the Hamming distance as the approximate distance. Product Quantization (PQ) on the other hand transforms the original vector into discrete, compact quantized codes using a pre-trained codebook. The distance computation of PQ can be accelerated via distance look-up based on a pre-computed look-up table, making it effective for distance computing. Due to the quantized nature of BQ and PQ, their distance computation can also be efficiently

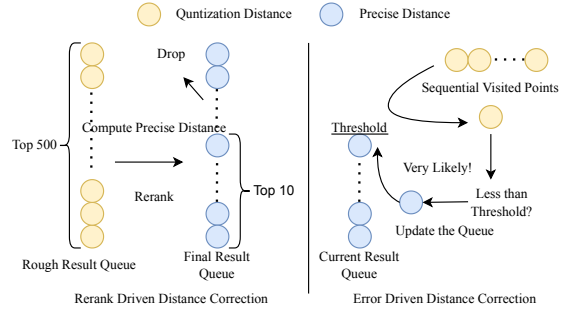


Figure 1: Example of Distance Correction Scheme

operated through hardware instruction sets such as SIMD [3, 22], thereby achieving extremely high search efficiency. However, a consequence of vector quantization is a significant drop in retrieval accuracy. According to a recent survey [50], no quantization method has achieved a 50% search recall on the SIFT dataset with 128 bits.

To address this issue, existing methods utilize re-ranking, which involves searching within a certain range for approximate nearest neighbors to calculate precise distances for reordering, or employ error bounds-driven methods to determine whether each distance calculation during retrieval requires the origin vector, thereby correcting the approximate distances computed by quantized vectors. The above distance correction scheme has been widely applied in both in-memory and disk-based AKNN searches. Specifically, the error bounds-driven distance correction successfully improves in-memory AKNN search efficiency by taking random projection as approximate distance [21] while the re-rank method is first used in DiskANN to reload origin vectors from disk and compute precise distance thereby improving search accuracy.

EXAMPLE 1. Fig. 1 illustrates the current two methods for distance correction. The re-rank method first searches the top 500 approximate nearest neighbors with quantized distance using an AKNN index such as IVF. Then compute the precise distance and re-sort the result with the new computed distances to obtain the top 20 nearest neighbors. The error-driven method uses error bounds to determine whether the precise distance is less than the result queue threshold with high probability. If so, the precise distance computation is needed to update the result queue.

However, the distance correction scheme driven by reranking and error bounds still has many issues. Firstly, the reranking method does not guarantee improved AKNN search accuracy after reordering; it requires manual adjustment of the reranking range multiple times to enhance AKNN search accuracy. At the same time, extensive reranking necessitates a significant amount of precise

distance calculations, greatly impacting AKNN search efficiency. Methods driven by error bounds, such as method based on random projection [21], experience a considerable error in distance estimation, and are not cache-friendly in hardware environments, making it difficult to leverage the potential of hardware instruction sets like SIMD. The current state-of-the-art quantization method RabitQ [22], which utilizes spatial geometric properties and error bounds for distance correction, requires the quantization bits to equal the vector dimensions. This means it can only use a fixed compression ratio of 32x or lower [22], limiting its flexibility.

In this paper, we consider more flexible AKNN search scenarios. We start by considering the distribution of data and observe that the variance of high-dimensional vectors, after being rotated by a PCA matrix, follows a long-tailed distribution. Based on this observation, we decompose the distance computation of vectors and design a multi-stage distance correction framework named Minimization Residual Quantization (MRQ), which involves three stages including quantization, projection, and full precise distance computation. Our method not only fully exploits the potential of quantization methods under hardware-accelerated instruction sets with more flexible quantization bit length making it more feasible for memory-limited AKNN search. But also takes advantage of projection methods to gradually accumulate dimension calculations for precise distance computation.

We summarize our main contribution as follows:

- *Data Distribution Analysis.* We analyzed the data distribution of the existing vector datasets. We observed that after the vector data is rotated by the PCA matrix, the variance of the dimensions exhibits a long-tail distribution. This also means that after the PCA projection, the distance calculation of most dimensions contributes limited to the overall distance. Thus, we can achieve the purpose of distance correction with fewer data dimensions.
- *New Distance Correction Method.* Based on the observations of data distribution, we designed a multi-stage distance correction method. We first decompose the computation of the Euclidean distance and design a multi-stage error-bound-driven distance correction method. Initially, we use binary quantization for the first stage of distance correction, followed by a secondary correction using the projected vectors, and finally, precise distance computation. Our designed multi-stage distance correction method not only adapts well to the hardware environment but also ensures the correction precision based on error bounds.
- *Efficient Implementation.* We have applied and adapted our method to the IVF-based AKNN index. By decomposing the data according to the multi-stage distance correction, we are able to optimize the data layout in memory more effectively, achieving a higher cache hit rate. Additionally, we have made further approximations to the IVF index, such as approximating the centroids of IVF, to enhance the search efficiency of the index further.
- *Extensive Experiment Analysis.* We evaluated our method on several real datasets and compared it with several state-of-the-art methods, such as the graph-based method HNSW and the quantization-based RabitQ, serving as baselines. Overall, our method surpasses the existing SOTA on multiple datasets, achieving up to 3x improvement in search efficiency at the same level of retrieval accuracy.

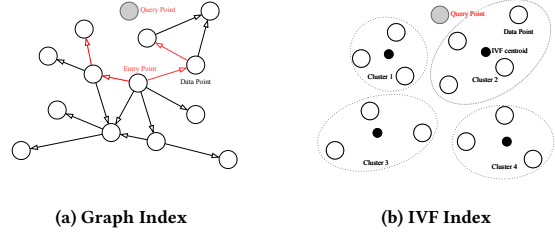


Figure 2: Examples of IVF and Graph Index

2 PRELIMINARY

In this section, we first introduce the problem definition of AKNN search and the existing approaches. Moreover, we also introduce the existing distance correction schemes and their combination with the AKNN index.

2.1 The AKNN Problem and Index

Given a database S consisting of n points in the D -dimensional Euclidean space \mathbb{R}^D , and a query point $q \in \mathbb{R}^D$. The object of the KNN (K-Nearest Neighbor) search is to find the top K points in S that are closest to the query vector q within Euclidean distance. Given the prohibitively high cost of KNN search in high-dimensional spaces [32], existing methods have shifted their focus towards Approximate K Nearest Neighbor (AKNN) search. Recall is a common metric utilized to evaluate the precision of the AKNN search algorithm. The definition of recall is the ratio of the KNN returned by the AKNN algorithm that are true K Nearest Neighbors, computed as follows:

$$\text{Recall}@K = \frac{|T \cap G|}{|G|}$$

where T is the set of AKNN algorithm returned, and G is the set of true KNN for the given query q . The goal of AKNN algorithms is to achieve higher recall with a lower computational cost. Consequently, numerous AKNN algorithms have been proposed, which can be mainly divided into four categories: methods based on hashing [13, 14, 19, 21, 24, 25, 30, 31, 49, 50, 58], methods based on quantization or inverted-file (IVF) [2, 5, 6, 22, 23, 26, 28, 36, 53, 57], methods based on trees [4, 7, 12, 15], and methods based on graphs [9, 17, 18, 29, 33, 41, 43, 44, 46].

Among the numerous AKNN indices, IVF and graph-based AKNN indices are the main focus of this paper due to their widespread application and state-of-the-art search efficiency.

IVF-based AKNN index first partition the space of vector data, specifically by clustering vector data using methods such as k-means to obtain cluster centroids, and then mapping each point to its nearest centroid. During the search stage, the nearest neighbors corresponding to the few centroids closest to the query are retrieved and their distances are calculated to obtain the k nearest neighbors. As shown on the right in Fig 2, when a query is given, the IVF index search points corresponding to the centroid and returns the KNN closest to the query.

Graph-based AKNN index views the points in high-dimensional space as nodes on a graph, with each node connected to vectors that are close to it, forming a graph with navigational properties. During

the search process, graph-based methods start from an entry point on the graph, moving step by step to neighbors closer to the query. If the search falls into a local optimum, it backtracks. As shown on the right in Figure 1, the search path on the graph is marked in red.

The common part between IVF and graph-based indexes lies in the use of a result queue with a fixed size (which can be considered a heap) to maintain the top K nearest neighbors during the search process. When using the re-rank method for distance correction, a larger queue size is required. On the other hand, when using error bounds, it is necessary to compare the error bound of the current approximate distance with the threshold of the result queue. We discuss the distance correction scheme further in section 2.3.

2.2 Vector Quantization

Vector quantization is widely applied in AKNN search to save storage costs and improve search efficiency. The core idea of vector quantization is to map vectors from a high-dimensional continuous space onto discrete codes. Among them, the product quantization (PQ) family and binary quantization (BQ) have been widely used in vector quantization due to their high compression ratio and efficient distance computation performance.

Product Quantization. Product Quantization (PQ) initially partitions the original vector space into multiple subspaces. For instance, a 128-dimensional vector is divided into 32 subspaces, each with 8 dimensions. Subsequently, clustering methods such as K-means are applied within these subspaces. Thus, the original vectors can be represented by the Cartesian product of centroids in each vector space. When calculating distances, PQ can utilize a look-up table to precompute and store the distances from the query to all centroids. The approximate distance to the query can then be obtained by simply summing the corresponding centroid distances, facilitating an efficient estimation of distances.

Binary Quantization. Binary Quantization (BQ) maps vectors into binary strings and uses the Hamming distance between binary strings as an approximation of the exact distance during AKNN search. For instance, Signed random projection [8] estimates angular values by generating binary codes through random projections. Iterative Quantization (ITQ) [26] transforms binary quantization into an optimization problem, which minimizes the mean square error between the binary codes and the original vectors through an orthogonal matrix. The recent approach, RabitQ [22], utilizes spatial geometric properties to unbiasedly estimate the inner product of vectors and correct the distance through the error bound.

Remark. Both BQ and PQ can accelerate distance calculation due to their quantization nature and reduction in vector dimensions. However, the BQ method can be directly computed using bitwise operators, which fits well with hardware acceleration instruction sets such as SIMD. On the other hand, the PQ method requires using techniques like 4-bit quantization [2] to fit the entire look-up table into SIMD registers, leading to larger quantization errors.

2.3 Distance Correction Scheme

Although vector quantization methods are highly effective in improving computational efficiency and reducing storage space in AKNN search, they often lead to a significant decrease in search accuracy (recall). To avoid a substantial drop in search accuracy, a

feasible approach is to use exact distances for correction in partial approximate distance computations [20–22, 33?]. The two popular existing methods are re-rank and error bounds driven distance correction.

Re-ranking. The idea of using re-rank for distance correction is simple: it first uses approximate distance for AKNN search and saves a larger range, such as Top R (where $R > K$), of approximate nearest neighbors. Then, it recomputes the exact distances for all vectors within this range and obtains the Top K nearest neighbor. The re-rank method is widely used in disk-based AKNN index [33, 51], where compressed vectors are stored in memory and full-precision vectors are stored on disk. When obtaining a temporary Top R nearest neighbor with approximate distance, the re-rank process loads the exact vectors from the disk and recomputes the distance to improve search accuracy.

Error Bounds. Through the analysis of error bounds of approximate distance methods, for example, the approximate distance obtained by random projection can be bounded by a multiplicative error bound of $(1 \pm \epsilon)$ compared to the precise distance with high probability according to the Johnson-Lindenstrauss lemma [16, 35]. We can leverage this error bound to determine whether the current approximate distance is less than the result queue threshold, thereby updating the AKNN result. If the lower bound of the approximate distance is greater than the maximum value in the current result queue, then there is no need for extra distance computation; otherwise, precise distance computation is required to update the result queue.

Discussion. Methods for improving AKNN search accuracy through distance correction, re-ranking, and error bound-based approaches essentially aim to obtain the precise distances to the k-nearest neighbors of the query. The key difference is that the method based on error bound provides guarantees on search accuracy, whereas the re-ranking method requires empirically setting the re-ranking range to achieve the desired AKNN search accuracy target.

3 PROBLEM ANALYSIS AND OBSERVATION

In this section, we discuss the main problem we focus on and the observation that motivates our technical method.

3.1 Problem Analysis

We begin our analysis with the SOTA quantization method RabitQ. RabitQ relies on random projection, where the original vector is centralized and then projected via a random orthogonal matrix P , normalized to a unit vector. Subsequently, it uses a random codebook composed to quantize only the direction of the vector. Specifically, the Euclidean distance can be reduced to an inner product computation by preprocessing to extract the norm term, i.e., $(\|\mathbf{x} - \mathbf{q}\| = \|\mathbf{x}\| + \|\mathbf{q}\| - 2 \cdot \langle \mathbf{x}, \mathbf{q} \rangle)$. RabitQ uses $\langle \tilde{\mathbf{x}}, \mathbf{q} \rangle / \langle \tilde{\mathbf{x}}, \mathbf{x} \rangle$ as an unbiased estimator to estimate $\langle \mathbf{x}, \mathbf{q} \rangle$, where $\tilde{\mathbf{x}}$ is the quantized vector of \mathbf{x} . The estimator requires the inner product of the quantized vector $\tilde{\mathbf{x}}$ and \mathbf{x} , which necessitates that the length of the binary string formed by the quantized vector is equal to the dimension of \mathbf{x} . When the vector is commonly stored using float32, this can achieve a fixed compression ratio of 32x.

A fixed compression ratio poses a challenge to search efficiency and memory-limited AKNN search schemes. Specifically, a fixed

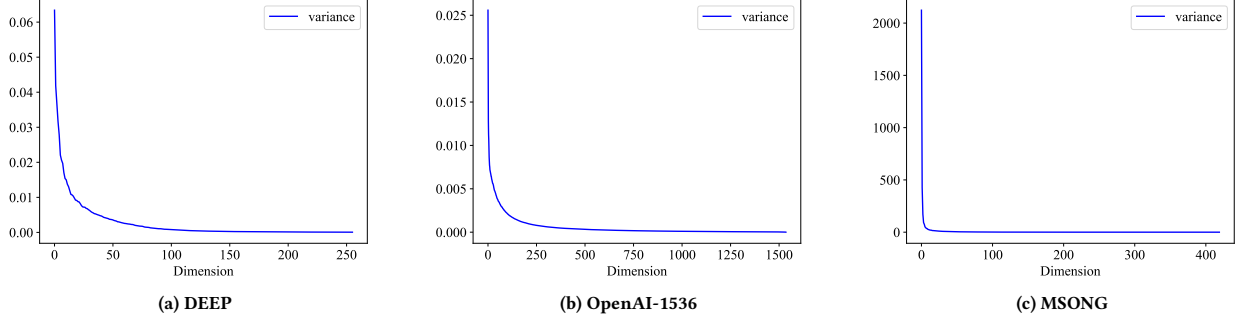


Figure 3: Examples of Vector Data Variance Distribution After PCA Transform

compression ratio may result in vectors compressed for disk storage not fitting into memory. For example, with 16GB of memory and 1TB of storage for vectors, only half of the quantized data can be loaded into memory. In terms of retrieval efficiency, binary strings of the same length as the vectors can lead to redundant operations with SIMD instruction sets, as the vector length may not be divisible by 64 or 128, thus reducing efficiency.

3.2 Observation

We then discuss two main observations that motivate our proposed approaches.

Data Distribution Analysis. We start our analysis with the vector data managed by vector databases. Existing vector data often consists of high-dimensional embeddings of audio, images, and text obtained using neural networks, typically exceeding 1000 dimensions. We found that after applying PCA, **the variance of the vector data follows a long-tailed distribution**.

EXAMPLE 2. As illustrated in Fig. 3, with data generated by the OpenAI-1536 text embedding model, the first 512 dimensions after PCA capture almost 90% of the variance, while the residual dimensions, nearly 1000, capture only about 10% of the variance. Other types of embeddings exhibit the same phenomenon, as the image embeddings from the Deep dataset and audio embeddings from the Msong dataset, after PCA rotation, only 128 dimensions are needed to retain 90% of the variance from the original data.

From an information theory perspective, greater variance in each dimension implies more information. This also means that only a few dimensions are needed to retain the majority of the information on the original vector. Analyzing from the error perspective, the smaller the variance in the residual dimensions, the smaller the mean squared error (MSE) when projecting to lower dimensions. Therefore, due to the lesser information and potentially smaller errors in the residual dimensions, we can consider discarding them during quantization.

Distance Computation Analysis. We then consider distance computation and correction techniques for quantization. Generally, for lower-dimensional data, such as the 128-dimensional Sift1B dataset which is stored as uint8, the cost of such distance computation consists of a smaller portion of the overall time cost compared to high-dimensional vector data over 1000 dimensions with float32

format. At the same time, according to recent datasets [20] and the latest AI embedding models [54], the data generated is basically thousands of dimensions, which makes distance calculation account for a larger proportion of AKNN searches.

However, the distance correction of highly accurate quantization **only requires a small number of precise distance computations with error bounds**. For example, in the GIST dataset, the RabitQ with IVF index requires only about 1% of distance computation to be precise under a 95% recall target, averaging around 200 exact distance computations per query, which is much smaller than the range required by the re-ranking method at the same level of precision.

4 MINIMIZED RESIDUAL QUANTIZATION

Based on the observation above, we consider a more flexible quantization with geometry relationship in this section that is not constrained by the dimensionality of the vectors. At the same time, the algorithm still needs to adapt to error-driven distance correction; therefore, we conducted further error analysis to ensure that it can utilize error bounds for distance correction.

4.1 Vector Decomposition

From the observation of the variance distribution of data dimensions after PCA projection, an intuitive idea is to project the data into a lower-dimensional space and then quantize the projected vectors. In this way, the compression ratio of vector quantization can be controlled by the dimensionality of the projection.

Specifically, consider a vector dataset S contain N points in D dimensional Euclidean space \mathbb{R}^D . The vector $\mathbf{x} \in S$ can be projected into a d -dimensional space ($d < D$) using an orthogonal matrix \mathbf{R} , that is, $\mathbf{x}_d = \mathbf{R}\mathbf{x}$. We can then apply the RabitQ quantization method to \mathbf{x}_d . Then the precise square Euclidean distance dis between database vector \mathbf{x} and query vector \mathbf{q} can be expressed as:

$$dis = \|\mathbf{x} - \mathbf{q}\|^2 = \|\mathbf{x}_d - \mathbf{q}_d\|^2 + \|\mathbf{x}_r - \mathbf{q}_r\|^2 \quad (1)$$

where \mathbf{x}_r is the vector residual dimension ($r + d = D$). RabitQ requires the vector to be normalized and centered. The projection distance $\|\mathbf{x}_d - \mathbf{q}_d\|^2$ can be further expressed, by letting \mathbf{c} be the centroid of the projection data \mathbf{x}_d , and the normalized projected vector will be $\mathbf{x}_b := \frac{\mathbf{x}_d - \mathbf{c}}{\|\mathbf{x}_d - \mathbf{c}\|}$. At the same time, the query vector is

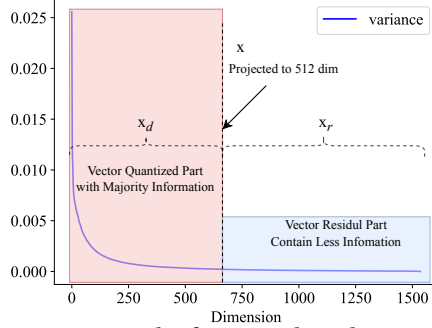


Figure 4: Example of Vector Split and Quantization

also projected and normalized where $q_b := \frac{q_d - c}{\|q_d - c\|}$. After normalizing, the projection distance $\|x_d - q_d\|^2$ can be converted to the combination of inner product and vector norm.

$$\begin{aligned} \|x_d - q_d\|^2 &= \|x_d - c\|^2 + \|q_d - c\|^2 \\ &\quad - 2 \cdot \|x_d - c\| \cdot \|q_d - c\| \cdot \langle x_b, q_b \rangle \end{aligned} \quad (2)$$

The projected inner product part $\langle x_b, q_b \rangle$ can be directly quantized by RabbitQ with d bits binary vector, only left the residual part $\|x_r - q_r\|^2$ require computation as the example illustrates in Fig. 1. The norm term of base vector x can be pre-computed and stored, the query norm only needs to be computed once for a single AKNN search. Then we also split the norm of residual dimension and get the equation:

$$\begin{aligned} \|x - q\|^2 &= \|x_d - c\|^2 + \|q_d - c\|^2 + \|x_r\|^2 + \|q_r\|^2 \\ &\quad - 2 \cdot \|x_d - c\| \cdot \|q_d - c\| \cdot \langle x_b, q_b \rangle - 2 \cdot \langle x_r, q_r \rangle \end{aligned} \quad (3)$$

The vector decomposition converts the Euclidean distance into the projection and the residual part. The empirical data distribution study shows the residual dimension only contains a small proportion of variance. Recent study [55] has proven that the residual dimension variance is minimized by the PCA matrix under orthogonal constrain. Then we can consider quantizing the PCA projection vector for inner product computation only to improve the flexibility and efficiency of RabbitQ.

4.2 Distance Approximation and Error Analysis

After the vector decomposition, we consider the distance approximation to maintain accuracy and efficiency. We set the norm part as $C_1 := \|x_d - c\|^2 + \|q_d - c\|^2 + \|x_r\|^2 + \|q_r\|^2$ the quantized part as $C_2 := -2 \cdot \|x_d - c\| \cdot \|q_d - c\| \cdot \langle x_b, q_b \rangle$, and residual part as $C_3 := -2 \cdot \langle x_r, q_r \rangle$. From the efficiency perspective, the base vector norm $\|x_d - c\|$ and $\|x_r\|$ can be pre-computed and store. Then the C_1 part only requires the computation of $\|q_d - c\|$ and $\|q_r\|$ which only computed once for a single query. With the vector norm pre-compute, the component of Euclidean distance after decomposition only left the inner product of $\langle x_b, q_b \rangle$ and $\langle x_r, q_r \rangle$. Then we study the vector quantization for efficient distance computing.

Vector Quantization. Note that the $\langle x_b, q_b \rangle$ is the inner product between two normalized vectors where $q_b := \frac{q_d - c}{\|q_d - c\|}$ and $x_b := \frac{x_d - c}{\|x_d - c\|}$. We can directly conduct the RabbitQ quantization to

estimate $\langle x_b, q_b \rangle$. Specifically, $\frac{\langle \bar{x}_b, q_b \rangle}{\langle \bar{x}_b, x_b \rangle}$ is prove to be good unbiased estimator of $\langle x_b, q_b \rangle$ where \bar{x}_b is the quantized vector of x based on a random rotate codebook C_{rand} , that is $C := \{-\frac{1}{\sqrt{D}}, +\frac{1}{\sqrt{D}}\}^D$ with random orthogonal rotate and get $C_{rand} := \{P\bar{x} | \bar{x} \in C\}$. With the $\langle x_b, q_b \rangle$ estimated by quantized vector $\frac{\langle \bar{x}_b, q_b \rangle}{\langle \bar{x}_b, x_b \rangle}$, the distance computation still left $\langle x_r, q_r \rangle$ for compute. From both empirical observation and theoretical analysis, the residual dimension contributes less to the entire vector distance computation. Then we directly omit the residual inner product and get the final approximate distance:

$$\begin{aligned} dis' &= \|x_d - c\|^2 + \|q_d - c\|^2 + \|x_r\|^2 + \|q_r\|^2 \\ &\quad - 2 \cdot \|x_d - c\| \cdot \langle x_b, q_b \rangle / \langle \bar{x}_b, x_b \rangle \end{aligned} \quad (4)$$

Error Analysis. Next, we study the approximate distance error (the gap between dis and dis') to obtain the error bound for distance correction. The error of approximate distance comes from two parts. First, the quantization of $\langle x_b, q_b \rangle$ leads the quantization error ϵ_q . Second, the omission of residual dimension brings the residual error ϵ_r . Fortunately, the vector data rotated by PCA becomes **independent** in each dimension. Then we can analyze the quantization error and residual error separately. Specifically, the error of the estimator $\frac{\langle \bar{x}, q \rangle}{\langle \bar{x}, x \rangle}$ is bound by a concentrate inequality as:

$$\mathbb{P} \left\{ \left| \frac{\langle \bar{x}, q \rangle}{\langle \bar{x}, x \rangle} - \langle x, q \rangle \right| > \sqrt{\frac{1 - \langle \bar{x}, x \rangle^2}{\langle \bar{x}, x \rangle^2}} \cdot \frac{\epsilon_0}{\sqrt{D-1}} \right\} \leq 2e^{-c_0\epsilon_0^2} \quad (5)$$

where ϵ_0 is a parameter controls the failure probability and c_0 is a constant factor [22]. Then we consider the distribution of $\langle x_r, q_r \rangle$, the PCA rotation makes the residual dimension variance minimized, then a straightforward idea is to use variance to bound this part of the value. Specifically, let σ_i be the standard deviation of each dimension of x , then the variance of $\langle x_r, q_r \rangle$ can be express as below:

$$\sigma^2 = \text{Var}(\langle x_r, q_r \rangle) = \sum_{i=d+1}^{i \leq D} q_i^2 \sigma_i^2 \quad (6)$$

With the variance computed, we can use Chebyshev's inequality¹ to get the residual error bound:

$$\mathbb{P}(|\langle x_r, q_r \rangle| \geq m \cdot \sigma) \leq \frac{1}{m^2} \quad (7)$$

The residual error and quantization error are both bound by corresponding concentrate inequality and are independent of each other. We can simply add them up as the new error bound of the MRQ for distance correction. Next, we can consider the integration of the MRQ with AKNN.

5 INTEGRATE WITH EXISTING INDEX

Among the various indices for AKNN search, IVF-based methods have gained wide adoption in many vector databases due to their relatively simple implementation and the tiny size of the index. In this section, we consider the implementation of MRQ and the integration with IVF.

¹we centroid x first to yield a mean of zero

Algorithm 1: MRQ Index

Input: The database raw vector set S and quantization bit d
Output: The IVF index \mathcal{I} ; The PCA matrix P_p ; The random matrix P_r ; The quantization code; The pre-compute results of $||\mathbf{x}_d - \mathbf{c}||$, $||\mathbf{x}_r||$ and $\langle \bar{\mathbf{x}}, \mathbf{x} \rangle$; The residual variance σ_i

- 1 Train PCA matrix P_p with database vector set S ;
- 2 Derive residual variance σ_i from PCA training process;
- 3 Rotate $\mathbf{x} \in S$ with P_p by $\mathbf{x}_p = P_p \mathbf{x}$;
- 4 Compute the residual vector norm $||\mathbf{x}_r||$ from \mathbf{x}_p ;
- 5 Take the first d -dimension of \mathbf{x}_p and get \mathbf{x}_d ;
- 6 Train IVF centroids \mathbf{c}_d and index \mathbf{x}_d to get \mathcal{I} ;
- 7 Normalized \mathbf{x}_d and quantized to $\bar{\mathbf{x}}_d$ with random matrix P_r ;
- 8 Compute $||\mathbf{x}_d - \mathbf{c}_d||$ and $\langle \bar{\mathbf{x}}, \mathbf{x} \rangle$;

5.1 Index Construct

We first investigate the construction of MRQ and its combination with IVF: the algorithm partitions the data into disjoint clusters with the centroid of the cluster as the index. We summarize the indexing process in algorithm 1.

Index Algorithm. We perform the PCA first on the original data to low-dimensional space and derive the residual dimension variance from the eigenvalue decomposition process (Line 1-2). Then we rotate the original dataset S and compute the residual vector norm (Line 3-4). We build the IVF index based on projected vectors next as our experimental findings show that the approximate centroids lead to the same performance as the exact index (Line 5). Then we quantized the projected vector with RabbitQ where the IVF centroid could also be used to centralize the projected data (Line 7-8). Note that we use the PCA-rotated vectors as our new base vectors since the Euclidean distance is preserved if the query vector is after the same operation.

5.2 Query Process

With the index construct, we consider the query process in both the in-memory AKNN search and disk-based AKNN search. The disk-based search loads the quantized vector and the IVF index in the memory leaving the full precise vector in the disk where the in-memory search loads all the data. We then summarize the query process in algorithm 2. The ϵ_0 controls the confidence interval of equation (5) and m controls the standard deviation count for Chebychev's inequality. Parameter N^{probe} controls the scanned cluster number to achieve a tradeoff between efficiency and accuracy.

Query Algorithm. The query process begins with the PCA rotation of the query vector \mathbf{q} (Line 1). Then the residual variance is computed for distance correction (Line 2-3). The projected query \mathbf{q}_d is further quantized to improve the efficiency of distance computing (Line 4-5). The IVF index sorts the cluster centroid according to the distance and scans the top N^{probe} cluster's vector to search the KNN of \mathbf{q} while a result queue (heap) Q is used to maintain the search result (Line 6-7). For each vector, we first compute the approximate distance based on the quantized vector and pre-compute result (Line 8). Then we check if the distance is less than the threshold with high probability (Line 9-11). If so, we compute the precise distance and update the result (Line 14-15).

Algorithm 2: MRQ Query

Input: The query vector \mathbf{q} ; Index \mathcal{I} ; N^{probe} ; Quantized vector $\bar{\mathbf{x}}_d$; Matrix P_p, P_r ; PCA data \mathbf{x}_p ; Error bound parameter ϵ_0 and m ; The pre-compute results of $||\mathbf{x}_d - \mathbf{c}||$, $||\mathbf{x}_r||$ and $\langle \bar{\mathbf{x}}, \mathbf{x} \rangle$; The residual variance σ_i

Output: The K nearest neighbor of \mathbf{q}

- 1 Rotate query vector with PCA matrix $\mathbf{q}_p = P_p \mathbf{q}$;
- 2 Take first d dimension of \mathbf{q}_p as \mathbf{q}_d and rest as \mathbf{q}_r ;
- 3 Compute residual variance σ by Equation (6) with \mathbf{q}_r and σ_i ;
- 4 Normalized and random rotate \mathbf{q}_d by P_r to obtain \mathbf{q}'_d ;
- 5 Quantized query \mathbf{q}'_d to $\bar{\mathbf{q}}$;
- 6 Result $Q \leftarrow \emptyset$;
- 7 **for** each $ID \in \mathcal{I}$ in top N^{probe} centroid to \mathbf{q}_d **do**
- 8 Compute the approximate distance dis' based on Equation 4;
- 9 $\tau \leftarrow$ threshold of result queue Q ;
- 10 $\epsilon_b \leftarrow$ RabbitQ error with ϵ_0 ; // Quantized Error
- 11 $\epsilon_r \leftarrow m \cdot \sigma$; // Residual Error
- 12 **if** $dis' - \epsilon_b - \epsilon_r < \tau$ **then**
- 13 **if** $dis'_0 - \epsilon_r < \tau$ **then**
- 14 compute $dis = ||\mathbf{x}_p, \mathbf{q}_p||^2$;
- 15 update queue Q with dis ;
- 16 **return** Q ;

Table 1: Dataset Statistics

Dataset	Dimension	Size	Query Size	Type
MSONG	420	992,272	200	Audio
GIST	960	1,000,000	1000	Image
DEEP	256	1,000,000	1000	Image
TINY	384	5,000,000	1000	Image
WORD2VEC	300	1,000,000	1000	Text
MSMARC	1024	1,000,000	1000	Text
OpenAI-1536	1536	999,000	1000	Text
OpenAI-3072	3072	999,000	1000	Text

Optimization. The distance computation can be further improved by only considering the residual error. Where $dis'_0 = ||\mathbf{x}|| + ||\mathbf{q}|| - 2 \cdot \langle \mathbf{x}_d, \mathbf{q}_d \rangle$ and with only the residual error. We can then simply add another prune condition $dis'_0 - m \cdot \sigma < \tau$ (Line 13) in algorithm 2 to further prune unnecessary distance computation. The memory layout can also be optimized as the approach in [21] to obtain a higher cache hit rate.

6 EXPERIMENT

6.1 Experiment Setting

Datasets. We use eight public datasets including datasets that are widely used in the benchmark (MSONG GIST DEEP TINY)² and the datasets generated from the latest embedding model (MSMARC³ OpenAI-1536⁴ OpenAI-3072⁵) to evaluate our method. All datasets

²<https://www.cse.cuhk.edu.hk/systems/hash/gqr/datasets.html>³<https://huggingface.co/datasets/Cohere/msmarco-v2.1-embed-english-v3>⁴<https://huggingface.co/datasets/Qdrant/dbpedia-entities-openai3-text-embedding-3-large-1536-1M>⁵<https://huggingface.co/datasets/Qdrant/dbpedia-entities-openai3-text-embedding-3-large-3072-1M>

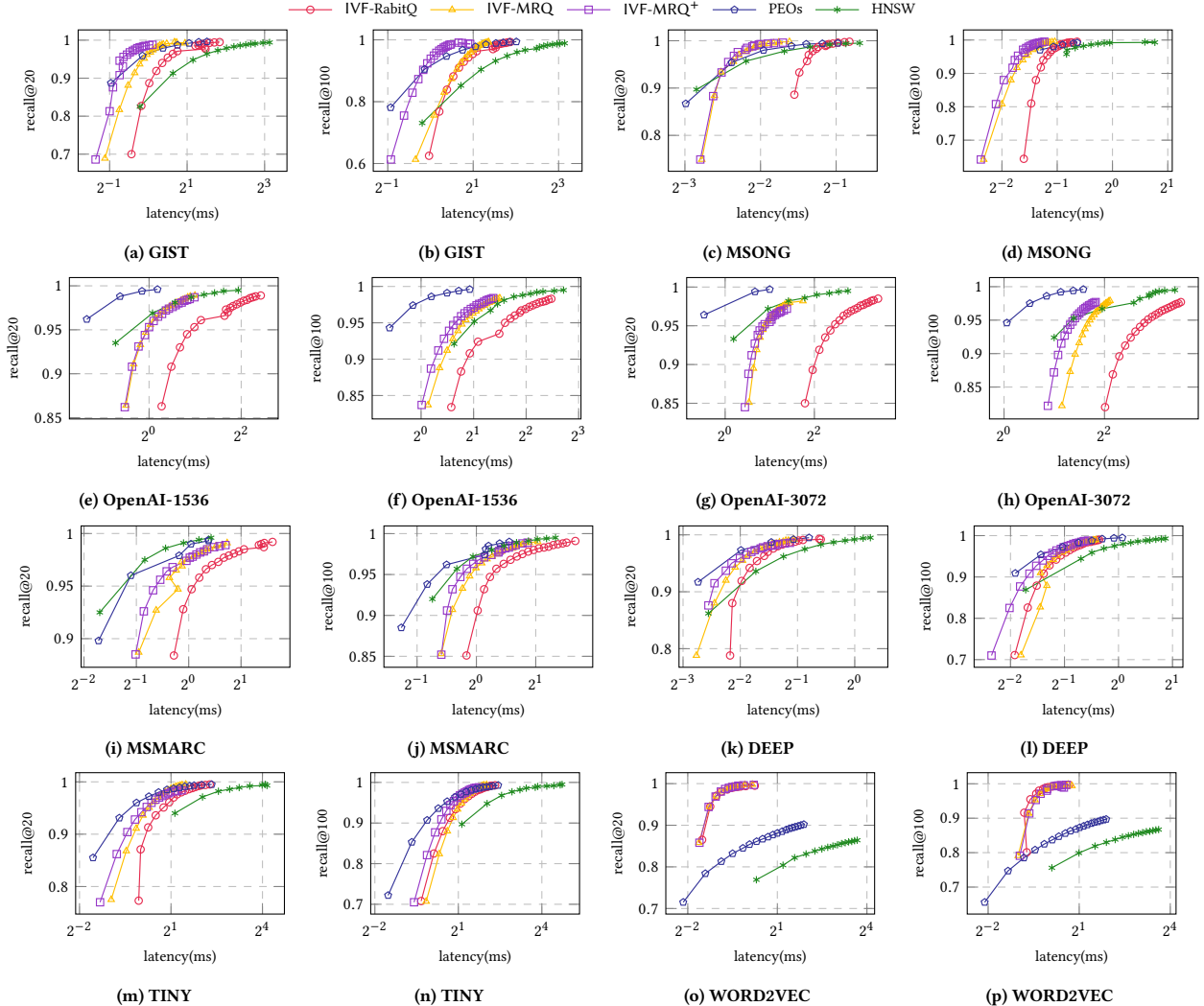


Figure 5: The Performance Test Among Various Method

detailed in Table 1, including the data size, query size, data dimension, and data types such as audio, image, and text. For datasets with no query vectors, we directly sample 1000 base vectors as queries and eliminate them to clear the base. All data in our experiments are stored in the float32 format.

Evaluation Metric We evaluate the accuracy of our method based on recall@K (see § 2) of AKNN search where the K is set as 20 and 100. For the efficiency evaluation metric, we use query latency, which is the time delay AKNN handles for a single query. Additionally, we evaluate the precise distance computation for a more in-depth understanding of our method. All metrics are reported as average over the entire query dataset.

Algorithm. Our AKNN search algorithm includes IVF-MRQ (see § 5), and IVF-MRQ⁺ the IVF with optimized distance correction and layout. We investigate both the graph-based and IVF AKNN indexes as baselines. All compared algorithms are listed below:

- IVF-RabitQ: IVF index with RabbitQ quantization;

- IVF-MRQ: IVF index with MRQ quantization;
- IVF-MRQ⁺: IVF index with MRQ and optimized layout;
- PEOs [42]: the SOTA In-memory AKNN index based on optimized HNSW [44];
- HNSW [44]: the most popular graph-based AKNN search index.

Index Configuration. We implement the MRQ approach with C++ using g++ version 11.4.0 with -Ofast optimization and core-march=naive to enable AVX instructor. The IVF centroid is set as 4096 as recommended by the Faiss library [34]. The quantization bits parameters of MRQ are set as 128 for MSONG, DEEP, and GIST datasets; and 512 for OpenAI-1536, OpenAI-3072, and MSMARC datasets. For the PEOs method, we use the parameter from the origin paper. The parameter `efcosntruct` controls the quality of the HNSW index used in PEOs, which is set as 1000, and parameter M controls the out-degree of HNSW, which is set as 32. For the origin HNSW algorithm, we set $M = 16$ and `efcosntruct = 500` according to its recommended parameters and recent benchmark [21, 22, 44].

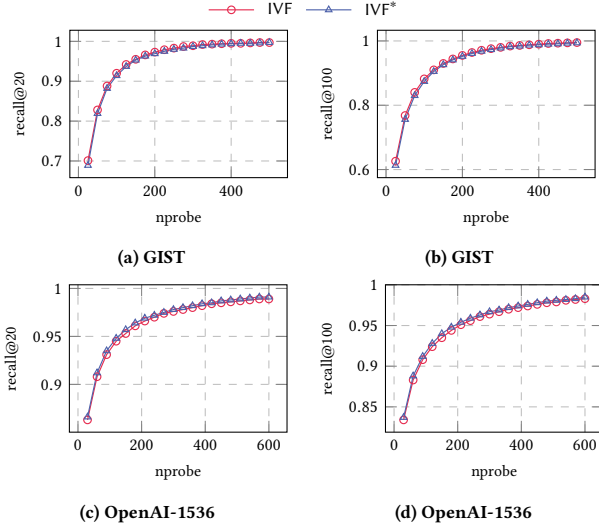


Figure 6: The Ablation Test of Index Approximation

6.2 Experiment Results

Exp-1: Performance Test. Fig. 5 shows the time-accuracy curve for all in-memory AKNN search algorithms, where the upper left indicates better performance. Our main findings reveal the following:

(1) Our distance computation method MRQ achieves a higher in-memory AKNN search efficiency while using fewer quantization bits than RabitQ. Specifically, our method uses only 1/7 of the quantization bits of RabitQ and achieves a 2x search latency reduction on the GIST dataset; use 1/3 bits and achieve a 2.6x latency reduction on OpenAI-1536 dataset; use 1/6 bits and achieve 3.4x latency reduction on OpenAI-3072 datasets.

(2) Our method is highly efficient in practice and surpasses the SOTA in-memory AKNN search algorithm. On the GIST dataset, our method achieves a 1.5x search latency reduction with previous SOTA method PEOs and a 5.85x latency reduction with origin HNSW at a high recall level. The PEOs method performs better on OpenAI-1536 and OpenAI-3072 datasets, prime due to the index structure where the HNSW index scanned fewer vectors than the IVF at the same recall. However, PEOs require several times index time and space than IVF and perform badly on the WORD2VEC dataset while our method is competitive on all datasets.

Exp-2: Ablation of Index Approximation We conduct an ablation study of the index approximation approach (see algorithm 1) by studying the precise centroid as an index and projected centroids as the approximation without considering the distance computation method (all use origin Euclidean distance). Fig. 6 shows the ablation results, where the x-axis represents the number of clusters scanned. The IVF marked in the red line indicates the origin centroid and IVF* marked in the blue line indicates the approximate approach. The IVF approach uses D dimension centroid, while the IVF* uses 128 dimensions for the GIST dataset (only the 1/7 of origin dimension) and 512 for the OpenAI-1536 dataset (1/3 of the origin dimension). As illustrated in Fig. 6, using projected centroid achieves almost no recall loss on the GIST dataset and performs

Table 2: Summary of Pre-processing Time(s)

	IVF-RabitQ	IVF-MRQ	HNSW	PEOs
MSONG	48	42	127	148
GIST	30	80	446	476
DEEP	31	37	47	155
TINY	147	130	563	1,729
WORD2VEC	37	45	32	86
MSMARC	88	115	133	381
OpenAI-1536	126	135	257	874
OpenAI-3072	235	115	503	1,709

Table 3: Summary of Index Size(MB)

	IVF-RabitQ	IVF-MRQ	HNSW	PEOs
MSONG	149	67	236	1,120
GIST	293	73	240	1,374
DEEP	97	67	237	1,540
TINY	590	280	1,139	6,750
WORD2VEC	115	101	237	717
MSMARC	307	181	240	2,308
OpenAI-1536	451	186	241	2,665
OpenAI-3072	890	229	247	2,955

slightly better on the OpenAI-1536 dataset. Thus, we used the projected centroid with our distance computation method. Meanwhile, the projected centroid also reduces the training time of the IVF index, making it efficient on large-scale datasets.

Exp-3: Pre-Processing Time and Space. We separately summarized all index processing times and spaces (without considering the base vector) of the compared algorithms in Table 2 and Table 3. The result shows that the index construction of our method is extremely fast and the index space requirement is almost negligible compared with HNSW and its optimized approach PEOs. Specifically, from the result in Table 2, the PEOs method requires 15x index time than our IVF-MRQ method on the OpenAI-3072 dataset and 13x index time on the TINY dataset. Moreover, our method requires only 1/2 of RabitQ, 1/4 of HNSW, and 1/24 of PEOs for space consumption on the TINY dataset and 1/14 of PEOs on the OpenAI-1536 dataset. Our algorithm has advantages in construction time and index size, which makes our algorithm more effective in resource-constrained scenarios.

7 CONCLUSION

In this paper, we propose a novel approach to achieve more flexible vector quantization, applying it to the vector distance computation part of high-dimensional AKNN search. By examining the data distribution, we decompose vectors into quantized and residual parts via projection and analyze the errors of both parts to facilitate distance correction. With the error analysis, we designed a multi-stage distance correction method to fully explore the potential for both the projection and quantization distance. Our experimental results demonstrate that our method can significantly enhance the efficiency of vector AKNN search while only requiring negligible index construct time and space.

REFERENCES

[1] Cecilia Aguerrebere, Mark Hildebrand, Ishwar Singh Bhati, Theodore Willke, and Mariano Tepper. 2024. Locally-Adaptive Quantization for Streaming Vector Search. *arXiv preprint arXiv:2402.02044* (2024).

[2] Fabien André, Anne-Marie Kermarrec, and Nicolas Le Scouarnec. 2015. Cache locality is not enough: High-Performance Nearest Neighbor Search with Product Quantization Fast Scan. *Proceedings of the VLDB Endowment* 9, 4 (2015).

[3] Fabien André, Anne-Marie Kermarrec, and Nicolas Le Scouarnec. 2019. Quicker adc: Unlocking the hidden potential of product quantization with SIMD. *IEEE transactions on pattern analysis and machine intelligence* 43, 5 (2019), 1666–1677.

[4] Ilias Azizi, Karima Echihabi, and Themis Palpanas. 2023. Elpis: Graph-based similarity search for scalable data science. *Proceedings of the VLDB Endowment* 16, 6 (2023), 1548–1559.

[5] Artem Babenko and Victor Lempitsky. 2014. Additive quantization for extreme vector compression. In *Proceedings of the IEEE Conference on Computer Vision and Pattern Recognition (CVPR)*, 931–938.

[6] Artem Babenko and Victor S. Lempitsky. 2015. The Inverted Multi-Index. *IEEE Trans. Pattern Anal. Mach. Intell.* 37, 6 (2015), 1247–1260.

[7] Alina Beygelzimer, Sham Kakade, and John Langford. 2006. Cover trees for nearest neighbor. In *Proceedings of the 23rd international conference on Machine learning*, 97–104.

[8] Moses S Charikar. 2002. Similarity estimation techniques from rounding algorithms. In *Proceedings of the thiry-fourth annual ACM symposium on Theory of computing*, 380–388.

[9] Patrick Chen, Wei-Cheng Chang, Jyun-Yu Jiang, Hsiang-Fu Yu, Inderjit Dhillon, and Cho-Jui Hsieh. 2023. FINGER: Fast Inference for Graph-based Approximate Nearest Neighbor Search. In *Proceedings of the ACM Web Conference 2023*, 3225–3235.

[10] Thomas Cover and Peter Hart. 1967. Nearest neighbor pattern classification. *IEEE transactions on information theory* 13, 1 (1967), 21–27.

[11] Xinyan Dai, Xiao Yan, Kelvin KW Ng, Jiu Liu, and James Cheng. 2020. Norm-explicit quantization: Improving vector quantization for maximum inner product search. In *Proceedings of the AAAI Conference on Artificial Intelligence*, Vol. 34, 51–58.

[12] Sanjoy Dasgupta and Yoav Freund. 2008. Random projection trees and low dimensional manifolds. In *Proceedings of the fortieth annual ACM symposium on Theory of computing*, 537–546.

[13] Mayur Datar, Nicole Immorlica, Piotr Indyk, and Vahab S Mirrokni. 2004. Locality-sensitive hashing scheme based on p-stable distributions. In *Proceedings of the twentieth annual symposium on Computational geometry*, 253–262.

[14] Yihe Dong, Piotr Indyk, Ilya P Razenshteyn, and Tal Wagner. 2020. Learning Space Partitions for Nearest Neighbor Search. *ICLR* (2020).

[15] Karima Echihabi, Panagiota Fatourou, Kostas Zoumpatianos, Themis Palpanas, and Houda Benbrahim. 2022. Hercules against data series similarity search. *Proceedings of the VLDB Endowment* 15, 10 (2022), 2005–2018.

[16] Casper Benjamin Freksen. 2021. An Introduction to Johnson-Lindenstrauss Transforms. *arXiv e-prints* (2021), arXiv-2103.

[17] Cong Fu, Changxi Wang, and Deng Cai. 2022. High Dimensional Similarity Search With Satellite System Graph: Efficiency, Scalability, and Unindexed Query Compatibility. *IEEE Trans. Pattern Anal. Mach. Intell.* 44, 8 (2022), 4139–4150.

[18] Cong Fu, Chao Xiang, Changxi Wang, and Deng Cai. 2019. Fast Approximate Nearest Neighbor Search With The Navigating Spreading-out Graph. *Proc. VLDB Endow.* 12, 5 (2019), 461–474.

[19] Junhao Gan, Jianlin Feng, Qiong Fang, and Wilfred Ng. 2012. Locality-sensitive hashing scheme based on dynamic collision counting. In *Proceedings of the 2012 ACM SIGMOD international conference on management of data*, 541–552.

[20] Jianyang Gao, Yutong Gou, Yuexuan Xu, Yongyi Yang, Cheng Long, and Raymond Chi-Wing Wong. 2024. Practical and Asymptotically Optimal Quantization of High-Dimensional Vectors in Euclidean Space for Approximate Nearest Neighbor Search. *arXiv preprint arXiv:2409.09913* (2024).

[21] Jianyang Gao and Cheng Long. 2023. High-Dimensional Approximate Nearest Neighbor Search: with Reliable and Efficient Distance Comparison Operations. *Proc. ACM Manag. Data* 1, 2 (2023), 137:1–137:27. <https://doi.org/10.1145/3589282>

[22] Jianyang Gao and Cheng Long. 2024. RaBitQ: Quantizing High-Dimensional Vectors with a Theoretical Error Bound for Approximate Nearest Neighbor Search. *Proceedings of the ACM on Management of Data* 2, 3 (2024), 1–27.

[23] Tiezheng Ge, Kaiming He, Qifa Ke, and Jian Sun. 2014. Optimized Product Quantization. *IEEE Trans. Pattern Anal. Mach. Intell.* 36, 4 (2014), 744–755.

[24] Aristides Gionis, Piotr Indyk, Rajeev Motwani, et al. 1999. Similarity search in high dimensions via hashing. In *Vldb*, Vol. 99. 518–529.

[25] Michel X Goemans and David P Williamson. 1995. Improved approximation algorithms for maximum cut and satisfiability problems using semidefinite programming. *Journal of the ACM (JACM)* 42, 6 (1995), 1115–1145.

[26] Yunchao Gong, Svetlana Lazebnik, Albert Gordo, and Florent Perronnin. 2013. Iterative Quantization: A Procrustean Approach to Learning Binary Codes for Large-Scale Image Retrieval. *IEEE Trans. Pattern Anal. Mach. Intell.* 35, 12 (2013), 2916–2929. <https://doi.org/10.1109/TPAMI.2012.193>

[27] Robert Gray. 1984. Vector quantization. *IEEE Assp Magazine* 1, 2 (1984), 4–29.

[28] Ruiqi Guo, Sanjiv Kumar, Krzysztof Choromanski, and David Simcha. 2016. Quantization-based fast inner product search. In *Artificial intelligence and statistics*. PMLR, 482–490.

[29] Ben Harwood and Tom Drummond. 2016. Fanng: Fast approximate nearest neighbour graphs. In *Proceedings of the IEEE Conference on Computer Vision and Pattern Recognition*, 5713–5722.

[30] Qiang Huang, Jianlin Feng, Qiong Fang, Wilfred Ng, and Wei Wang. 2017. Query-aware locality-sensitive hashing scheme for lp norm. *The VLDB Journal* 26, 5 (2017), 683–708.

[31] Qiang Huang, Jianlin Feng, Yikai Zhang, Qiong Fang, and Wilfred Ng. 2015. Query-aware locality-sensitive hashing for approximate nearest neighbor search. *Proceedings of the VLDB Endowment* 9, 1 (2015), 1–12.

[32] Piotr Indyk and Rajeev Motwani. 1998. Approximate nearest neighbors: towards removing the curse of dimensionality. In *Proceedings of the thirtieth annual ACM symposium on Theory of computing*, 604–613.

[33] Suhas Jayaram Subramanya, Fnu Devvrit, Harsha Vardhan Simhadri, Ravishankar Krishnamamy, and Rohan Kadekodi. 2019. Diskann: Fast accurate billion-point nearest neighbor search on a single node. *Advances in Neural Information Processing Systems* 32 (2019).

[34] Jeff Johnson, Matthijs Douze, and Hervé Jégou. 2019. Billion-scale similarity search with GPUs. *IEEE Transactions on Big Data* 7, 3 (2019), 535–547.

[35] William B Johnson, Joram Lindenstrauss, and Gideon Schechtman. 1986. Extensions of Lipschitz maps into Banach spaces. *Israel Journal of Mathematics* 54, 2 (1986), 129–138.

[36] Yannis Kalantidis and Yannis Avrithis. 2014. Locally optimized product quantization for approximate nearest neighbor search. In *Proceedings of the IEEE conference on computer vision and pattern recognition*, 2321–2328.

[37] Weihao Kong and Wu-Jun Li. 2012. Isotropic hashing. *Advances in neural information processing systems* 25 (2012).

[38] Patrick Lewis, Ethan Perez, Aleksandra Piktus, Fabio Petroni, Vladimir Karpukhin, Naman Goyal, Heinrich Küttler, Mike Lewis, Wen-tau Yih, Tim Rocktäschel, et al. 2020. Retrieval-augmented generation for knowledge-intensive nlp tasks. *Advances in Neural Information Processing Systems* 33 (2020), 9459–9474.

[39] Jinfeng Li, Xiao Yan, Jian Zhang, An Xu, James Cheng, Jie Liu, Kelvin KW Ng, and Ti-chung Cheng. 2018. A general and efficient querying method for learning to hash. In *Proceedings of the 2018 International Conference on Management of Data*, 1333–1347.

[40] Ying Liu, Dengsheng Zhang, Guojun Lu, and Wei-Ying Ma. 2007. A survey of content-based image retrieval with high-level semantics. *Pattern recognition* 40, 1 (2007), 262–282.

[41] Kejing Lu, Mineichi Kudo, Chuan Xiao, and Yoshiharu Ishikawa. 2021. HVS: Hierarchical Graph Structure Based on Voronoi Diagrams for Solving Approximate Nearest Neighbor Search. *Proc. VLDB Endow.* 15, 2 (2021), 246–258.

[42] Kejing Lu, Chuan Xiao, and Yoshiharu Ishikawa. [n.d.]. Probabilistic Routing for Graph-Based Approximate Nearest Neighbor Search. In *ICML 2024*.

[43] Yury Malkov, Alexander Ponomarenko, Andrey Logvinov, and Vladimir Krylov. 2014. Approximate nearest neighbor algorithm based on navigable small world graphs. *Inf. Syst.* 45 (2014), 61–68.

[44] Yury A. Malkov and Dmitry A. Yashunin. 2020. Efficient and Robust Approximate Nearest Neighbor Search Using Hierarchical Navigable Small World Graphs. *IEEE Trans. Pattern Anal. Mach. Intell.* 42, 4 (2020), 824–836.

[45] Nasser M Nasrabadi and Robert A King. 1988. Image coding using vector quantization: A review. *IEEE Transactions on communications* 36, 8 (1988), 957–971.

[46] Yun Peng, Byron Choi, Tsz Nam Chan, Jianye Yang, and Jianliang Xu. 2023. Efficient Approximate Nearest Neighbor Search in Multi-dimensional Databases. *Proc. ACM Manag. Data* 1, 1 (2023), 54:1–54:27. <https://doi.org/10.1145/3588908>

[47] Maxim Raginsky and Svetlana Lazebnik. 2009. Locality-sensitive binary codes from shift-invariant kernels. *Advances in neural information processing systems* 22 (2009).

[48] JBen Schafer, Dan Frankowski, Jon Herlocker, and Shilad Sen. 2007. Collaborative filtering recommender systems. In *The adaptive web: methods and strategies of web personalization*. Springer, 291–324.

[49] Yifang Sun, Wei Wang, Jianbin Qin, Ying Zhang, and Xuemin Lin. 2014. SRS: Solving c-Approximate Nearest Neighbor Queries in High Dimensional Euclidean Space with a Tiny Index. *Proc. VLDB Endow.* 8, 1 (2014), 1–12.

[50] Jingdong Wang, Ting Zhang, Nicu Sebe, Heng Tao Shen, et al. 2017. A survey on learning to hash. *IEEE transactions on pattern analysis and machine intelligence* 40, 4 (2017), 769–790.

[51] Mengzhao Wang, Weizhi Xu, Xiaomeng Yi, Songlin Wu, Zhangyang Peng, Xiangyu Ke, Yunjun Gao, Xiaoliang Xu, Rentong Guo, and Charles Xie. 2024. Starling: An I/O-Efficient Disk-Resident Graph Index Framework for High-Dimensional Vector Similarity Search on Data Segment. *Proc. ACM Manag. Data* 2, 1 (2024), V2mod14:1–V2mod14:27. <https://doi.org/10.1145/3639269>

[52] Mengzhao Wang, Xiaoliang Xu, Qiang Yue, and Yuxiang Wang. 2021. A comprehensive survey and experimental comparison of graph-based approximate nearest neighbor search. *Proceedings of the VLDB Endowment* 14, 11 (2021), 1964–1978.

[53] Runhui Wang and Dong Deng. 2020. DeltaPQ: lossless product quantization code compression for high dimensional similarity search. *Proceedings of the VLDB Endowment* 13, 13 (2020), 3603–3616.

[54] Jasper Xian, Tommaso Teofili, Ronak Pradeep, and Jimmy Lin. 2024. Vector search with OpenAI embeddings: Lucene is all you need. In *Proceedings of the 17th ACM International Conference on Web Search and Data Mining*. 1090–1093.

[55] Mingyu Yang, Jiabao Jin, Xiangyu Wang, Zhitao Shen, Wei Jia, Wentao Li, and Wei Wang. 2024. *Technical Report*. github.com/mingyu-hkustgz/Res-Infer

[56] Qiang Yue, Xiaoliang Xu, Yuxiang Wang, Yikun Tao, and Xuliyuan Luo. 2024. Routing-Guided Learned Product Quantization for Graph-Based Approximate Nearest Neighbor Search. In *2024 IEEE 40th International Conference on Data Engineering (ICDE)*. IEEE, 4870–4883.

[57] Ting Zhang, Chao Du, and Jingdong Wang. 2014. Composite quantization for approximate nearest neighbor search. In *International Conference on Machine Learning*. PMLR, 838–846.

[58] Bolong Zheng, Xi Zhao, Lianggui Weng, Nguyen Quoc Viet Hung, Hang Liu, and Christian S. Jensen. 2020. PM-LSH: A Fast and Accurate LSH Framework for High-Dimensional Approximate NN Search. *Proc. VLDB Endow.* 13, 5 (2020), 643–655.